

GenHeld: Generating and Editing Handheld Objects

Chaerin Min¹

Srinath Sridhar^{1*}

¹Brown University

¹{chaerin_min, srinath_sridhar}@brown.edu

<https://ivl.cs.brown.edu/research/genheld.html>



Figure 1: We present GenHeld, a model to synthesize held objects given 3D hand model or 2D hand image. GenHeld3D can select plausible and diverse objects from a large object repository [19], while GenHeld2D can add or replace existing held objects in images.

Abstract

Grasping is an important human activity that has long been studied in robotics, computer vision, and cognitive science. Most existing works study grasping from the perspective of synthesizing hand poses conditioned on 3D or 2D object repre-

*Corresponding Author

sentations. We propose GenHeld to address the inverse problem of synthesizing held objects conditioned on 3D hand model or 2D image. Given a 3D model of hand, GenHeld3D can select a plausible held object from a large dataset using compact object representations called *object codes*. The selected object is then positioned and oriented to form a plausible grasp without changing hand pose. If only a 2D hand image is available, GenHeld2D can edit this image to add or replace a held object. GenHeld2D operates by combining the abilities of GenHeld3D with diffusion-based image editing. Results and experiments show that we outperform baselines and can generate plausible held objects in both 2D and 3D. Our experiments demonstrate that our method achieves high quality and plausibility of held object synthesis in both 3D and 2D.

1 Introduction

Touching, grasping, and manipulating objects constitute a majority of human interactive activities. Each day, we touch an average of 821 surfaces [31] and 140 different objects [104], enabling us to shape our environments to achieve our physical goals. Understanding how humans grasp objects can have profound impact in areas like robotics and mixed reality. Unsurprisingly, this important skill has long been a topic of study in robotics [7, 40, 45, 46, 74, 83, 87, 88], computer vision [12, 23, 39, 62, 94, 98], and cognitive science [89, 90].

The focus of most existing work that studies human grasps has been on synthesizing plausible or stable grasping hand poses conditioned on 3D object models [16, 30, 33, 34, 38, 44, 46, 58, 63, 79, 81, 82, 96, 98, 100, 101], or 2D hand images [21, 50, 56, 94]. In this problem setting, the object is assumed to be known, and the goal is to generate hand pose and/or shape parameters [72] that result in a plausible grasp. Some methods focus on synthesizing *both the hand and the object*, using conditioning [5, 12, 17, 39, 47, 62, 95]). While these methods have useful applications, they cannot support newly emerging applications. For instance, in virtual reality, we may want to automatically synthesize 3D held objects based on user’s hand pose/shape [4, 51]. In generative image editing, we may want to edit an image of a hand [62] to either add or replace a (held) object.

To support these emerging applications, we consider the inverse problem: *given a 3D model or 2D image of a hand (either free or holding another object), could we synthesize a **held object** that fits the input hand pose?* This previously underexplored [66] problem setting is highly challenging. First, the space of 3D object variation is significantly larger than that of hands, making it hard to synthesize plausible and diverse objects. Second, the contact and occlusions, and the requirement to keep hand pose unchanged, make it challenging to synthesize accurate held objects. Finally, despite incredible progress in image editing [9, 28, 35, 52, 61, 71, 75, 92], generating realistic images of hands and grasps has been found to be particularly hard [1, 2] (see Figure 2).

To address these challenges, we present **GenHeld**, a method that synthesizes 3D or 2D **held objects** conditioned on a 3D hand model or a 2D image of a hand. Given the 3D pose and/or shape of a hand (e.g., MANO [72]), our **GenHeld3D** module is capable of selecting a plausible held object from the large and diverse Objaverse dataset [19], and posing the object so that the hand grasps it without articulation changes. To enable this, GenHeld3D consists of an object selection network that is trained on a dataset of grasps [13] to generate **object codes** – compact representations of the geometry of plausible held objects. These codes are then matched to objects in the Objaverse dataset to select a suitable held object. To ensure that the selected held objects can be grasped without change in hand pose, we introduce an object fitting procedure that optimizes for contacts, interpenetration, and physical laws.

If only a 2D image of a hand, either free or holding an object, is available, we can still handle it with **GenHeld2D**. GenHeld2D builds on top of GenHeld3D, but combines it with the editing capabilities of diffusion models [71]. Given a hand image, we first extract 3D pose and shape [41, 102] and use GenHeld3D to generate a plausible 3D held object. The 3D hand and generated held object are used as 3D guidance for a diffusion-based image editing process to add or replace existing held objects in the input image (see Figure 1).

We compare 3D grasp quality, object plausibility, and 2D editing plausibility of our method with related work. We show that the ability to select the plausible object greatly improves the 3D grasping quality, and leads to faster convergence in the object fitting. The capability of using an occlusion-

aware 3D grasp as guidance demonstrates superior 2D editing plausibility over not using such guidance (e.g., guided by text). To summarize our contributions:

- We study a previously underexplored grasping problem: given a 3D model or 2D image of a hand, we want to synthesize a **held object** that fits the input hand pose.
- We introduce **GenHeld3D**, a module that selects a plausible 3D held object from a large and diverse dataset using object codes and ensures physical grasp plausibility.
- We introduce **GenHeld2D**, a module that can add or replace to an image of a hand by combining the editing capabilities of diffusion models with GenHeld3D.

2 Related Works

Grasp Synthesis. Grasp synthesis refers to the task of generating either pose of a human or robot hand such that an object is grasped. In computer vision and graphics, the focus of grasp generation has been on plausible grasps that make accurate contact, without interpenetration, and physically correct [16, 33, 34, 79, 82, 91, 100, 101]. In robotics, however, the focus has been more on *stable grasps* that result in objects being successfully grasped in simulation or the real world [40, 74, 83, 86–88]. Many methods take 3D object representations as input for grasp synthesis [16, 33, 34, 38, 44, 46, 79, 82, 96, 98, 100, 101]. Heuristics [54] and physical simulation [16, 33, 82] are common ways of optimizing for stable grasps at inference time. ContactGen [44] predicted plausible contacts on objects, while HOIDiffusion [98] generated new images from synthesized grasps. Other approaches take an image as input and generate hands on the 2D image [62, 94, 95]. The proliferation of large language models has also inspired methods to generate hands grasping objects from text prompts [12, 17, 39].

Numerous datasets [24, 32, 43, 87], simulation environments [42, 54], and hand/objects datasets [11, 55, 72] have enabled research in grasp synthesis. This has enabled the study of real-world grasps with one hand [13], two hands [6, 8, 20, 23, 78], or robot hands [46] approaching and finally grasping objects. In this paper, we take advantage of the DexYCB [13] to learn object codes that enable us to select suitable objects from a large dataset [19]. The grasping studies also get much attention from robot grippers and the full-body motion generation. For robotics applications, [40, 83, 86, 88] considered physical laws and experimented on simulators. One such physics-aware approach [45] allows the grasping simulation to be differentiable, by formulating the force closure loss. We integrate this method in our object fitting procedure.

Some previous work integrate the entire body in the grasping process [66, 78–80, 91]. Object Pop-up [66] is a closely related work that generates plausible objects given a 3D point clouds of entire human body. However, our work differs in that we can generate more accurate contacts of objects from only 3D hand models. Furthermore, we also support direct editing of 2D hand images.

Image Editing. Editing images is a long-standing problem. For the object pasting and blending task, classical works included the famous alpha blending [85] and poisson blending [65]. Recently, the quality of image generation diffusion models [28, 29, 75] has enabled realistic editing capabilities. Such models include object resizing [61, 73], moving [59, 61, 64, 73], removal [61, 73], variation [61], and editing by text [9, 26, 35].

In this paper, we use GenHeld3D to generate plausible 3D objects and 3D hand pose/shape to guide editing of the original image. This leads us to focus on the object pasting which accepts reference image and source image. Paint-by-Example [92] and DiffEditor [60] support such object pasting. Paint-by-Example [92] allows changes in the reference image so that it can semantically harmonizes with the source image. On the other hand, DiffEditor [60] leverages the DDIM inversion [75] and score-based guidance [76, 77] with SDE [29] to balance between flexibility and preservation. Some



Figure 2: Stable Diffusion [71] struggles to edit images of hands holding objects. For an identity inpainting task (purple region), it is unable to faithfully reconstruct the hand or held object.

methods focus on editing images, using text prompts only. Imagic [35] edits real images, based on the text description of the edited result. InstructPix2Pix [9] edits real images with only the prompt about the edited part. While these methods can perform image editing, using only the text prompts may lead to difficulties in a particular problem – editing held objects. In experiments, we show that the GenHeld2D (combining the GenHeld3D into the existing object pasting pipeline) leads to better results than these methods. Notably, many of the aforementioned image editing techniques are general-purpose models, and thus are not naturally guided by any additional priors, e.g., 3D shapes and the hand template models [41, 72]. On the contrary, our approach is specifically designed for the hand grasping setting.

3 Method

Our proposed method, GenHeld, is designed to support two main tasks. GenHeld 3D takes 3D hand pose/shape as input and produces a plausible 3D held object. GenHeld 2D takes a hand image as input and edits the image to add or replace a held object using 3D guidance from GenHeld 3D. In the following sections, we describe each module in detail.

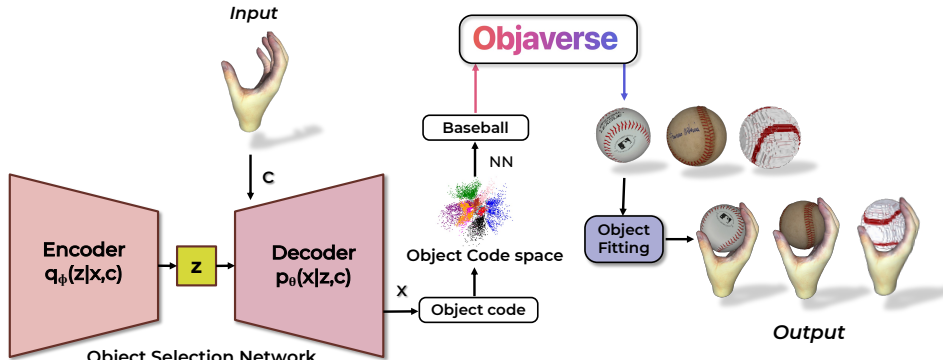


Figure 3: GenHeld3D can synthesize a 3D held object given a 3D hand model as input (top). We encode the 3D hand model to estimate **object codes** that act as a compact representation of plausible held objects. These object codes can be used to retrieve diverse objects from a much larger dataset like Objaverse [19]. This is followed by an object fitting step to position and orient objects to form the grasp without changing the initial hand pose.

3.1 GenHeld3D

When given a 3D hand model (pose and shape) as input, the goal of GenHeld 3D is to select an appropriate object from a large dataset of objects and pose it in a plausible grasp without changing the pose of the hand. To achieve this, we split the task into two parts: object selection and object fitting.

Object Selection. Synthesizing plausible and diverse objects corresponding to an input hand requires learning from real-world grasps of objects. However, existing grasp datasets [6, 13, 20, 23, 32, 46, 78, 86, 87] are limited in the diversity of held objects. We seek to select plausible and diverse held objects from large object datasets like Objaverse [19]. To achieve this, our main insight is to learn **object codes** – low-dimensional encodings of the object shapes from existing grasp datasets which can guide the selection of objects from a large object database.

We define an object code as $\mathbf{x} = [\frac{l_3}{b}, \frac{l_2}{l_3}, \frac{l_1}{l_2}]$, where l_i are the three lengths of tight 3D object bounding box. l_i are obtained by extracting principal components [3] of object vertex positions, and sorted to ensure the rotational invariance. We also define principal bone length b as the distance between root and the first joint of thumb, defined in MANO [72]. We aim to learn the distribution of \mathbf{x} from the 20 object categories [10] in a dataset of real hand grasps [13]. We can then use the learned object code distribution to find nearest matching category in a larger dataset [19] and sample diverse instances from that category. Since datasets like Objaverse can have object instances with arbitrary scales, we can rescaling the bounding box lengths of the fetched object as $l_1 = x_1 b, l_2 = x_1 x_2 b, l_3 = x_1 x_2 x_3 b$. Figure 4 visually describes the object selection procedure.

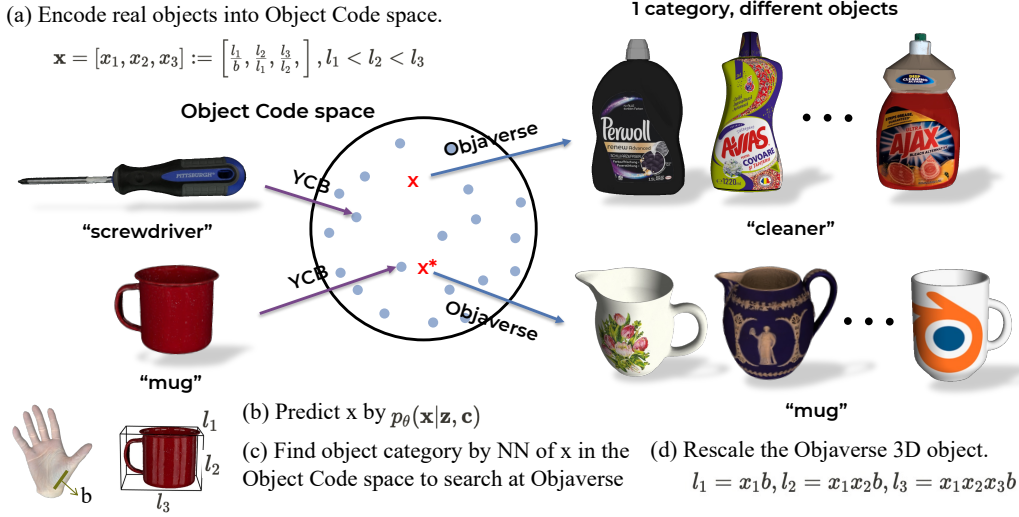


Figure 4: We use **object codes** – compact representations of object shapes learned from a real dataset of grasps. These codes can be used to find suitable diverse objects in a larger object dataset like Objaverse. Our method can also handle scale variations by normalizing using principal bone length b .

Predicting Object Codes. Our main insight is that object codes are associated with hand pose/shape. Thus, it should be possible to learn the association between 3D hand models and object code from existing grasp datasets. To do this, we build an object selection network (see Figure 14) that predicts object codes from an 3D hand pose and shape (vertices) and outputs object code and 3D contacts \mathbf{h}_c . We find that the contact plays an important role, because it is in the intersection between hand and object is made by contact. During training, a point cloud of the object shape, ground truth object codes and contact are provided as supervision. Please see the supplementary document for more details.

In summary, we try to bridge the object shape code generation task with hand pose, object, and contact. Shape code, object point clouds, and contact is supervised during training. For the ground truths, we acquire the paired data from an external dataset [13]. Also, we acquire the h_c^* by thresholding the distance between the vertices of hand and the object. The network is trained by the loss $\mathcal{L}_{\text{select}} = \mathcal{L}_{\text{rec}} + \lambda_{\text{KL}} \cdot \mathcal{L}_{\text{KL}}$, and \mathcal{L}_{rec} is given by,

$$\mathcal{L}_{\text{rec}} = \|\mathbf{x} - \mathbf{x}^*\|_2 + \lambda_o \cdot \|O - O^*\|_2 + \lambda_{\text{con}} \cdot \text{BCE}(\mathbf{h}_c, \mathbf{h}_c^*), \quad (1)$$

where $*$ denotes the ground-truths. λ controls the balances between losses. The KL divergence term is given by,

$$\mathcal{L}_{\text{KL}} = \text{KL}[\mathcal{N}(\mu_{\mathbf{z}}, \Sigma_{\mathbf{z}}^2) \| \mathcal{N}(0, I)]. \quad (2)$$

We apply an annealing strategy [48, 99] to \mathcal{L}_{KL} in order to avoid posterior collapse. During inference, we sample a latent vector \mathbf{z} to feed the decoder p_θ .

Object Fitting. When the fine-grained 3D object is fetched from Objaverse [19], our method tries to fit the object to the given hand. Note that the hand should be preserved, so only the object pose should be optimized. To achieve this, we incorporate multiple losses that control contact, penetration, and physical laws. We optimize the object transformation using the following loss function

$$\mathcal{L}_{\text{opt}} = \lambda_A \mathcal{L}_A + \lambda_R \mathcal{L}_R + \lambda_{\text{sim}} \mathcal{L}_{\text{sim}}, \quad (3)$$

where λ controls the strengths between terms. The attraction loss \mathcal{L}_A , and repulsion loss \mathcal{L}_R are given as,

$$\mathcal{L}_A = \sum_{i=1}^6 \Phi_\alpha(d(C_i \cap \text{PENE}_{\mathbf{h}}(V_{\text{obj}})^c, V_{\text{obj}})), \quad \mathcal{L}_R = \sum_{v \in \text{PENE}_{\mathbf{h}}(V_{\text{obj}})} \Phi_\alpha(d(v, V_{\text{obj}})). \quad (4)$$

We follow the specific formulation produced by [24], but we only allow object translation, rotation, and scaling as variables. The object scaling is wrapped by a Sigmoid function to avoid scale explosion,

as $s(x) = \frac{2k}{1+\exp(-x+1)} + 1 - k$, where we allow the max scale to be $1 + k$ and min scale to be $1 - k$. We use the common penalization function $\Phi_\alpha(x) = \alpha \tan(\frac{x}{\alpha})$ with the characteristic distance action α . The $C = \{C_i\}, i \in [1, 6]$ is given by the statistical set of contact vertices from [24]. The minimum distance between a vertex point and a set of vertices is defined as $d(v, V) = \inf_{w \in V} \|v - w\|_2$, and the minimum distance between the two sets of vertices is given by $d(\tilde{V}, V) = \inf_{v \in \tilde{V}} d(v, V)$. Plus, we compute the penetration (PENE) with the classic Ray-Triangle intersection [57] for better efficiency. Inspired by the Differentiable Force Closure [18, 45], we also enforce the physical plausibility using a differentiable simulation loss \mathcal{L}_{sim} . This makes sure the forces exerted on the object is closed, so that the object will not fall down. Please see more details in the supplementary Appendix D.

3.2 GenHeld2D

While GenHeld3D can generate held objects given 3D hand model, we often may need to add or replace held objects in a hand image. We show how GenHeld3D can be combined with the editing capabilities of diffusion models to build GenHeld2D that operates directly on images (see Figure 5).

3D Guiding. The first step in operating on images is to obtain a 3D hand model corresponding to the input image. We then use this to generate a 3D held object using GenHeld3D. As shown in Figure 5, we first project the result of GenHeld3D onto the source image. Since the hand and object were defined in 3D, we can benefit from the pixel-wise information about the z-buffer. That means we can render the hand and object, either together, independently, or separately in a occlusion-aware way. This allows us to rectify the potential misalignment by leveraging the hand 2D keypoints from the independently projected hand. Also, such information on z-buffer enables to render only the un-occluded object parts onto the source image. By doing this, we can obtain the reference image, as depicted in Figure 5.

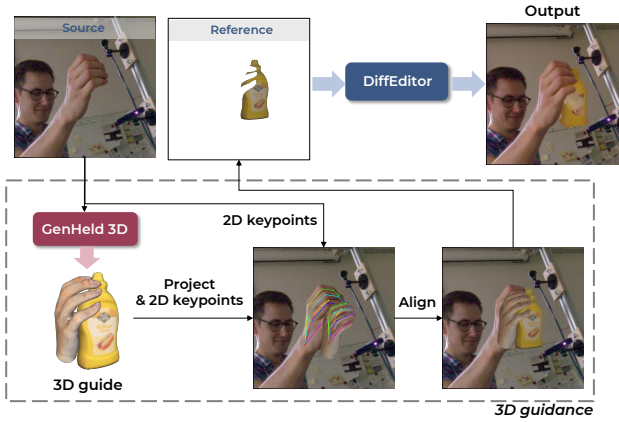


Figure 5: GenHeld2D enables us to add or replace held objects to 2D hand images. We do this by first lifting hand images to 3D hand and object using GenHeld3D. This is then following by 2D keypoint projection and alignment to create a 3D guidance image that is used to edit the image.

Object Pasting. Since GenHeld3D is able to provide a 3D guidance in the form of occlusion-aware grasped object and the source image. We then use, DiffEditor, a state-of-the-art object pasting model [60] without needing any training or fine-tuning. First, we perform DDIM Inversion [75] on both the source and reference image. This process produces keys and queries of those real images, which are fed into the cross attention module. Additionally, we guide the reverse process by the score-based function $\nabla_{x_t} \log q(x_t|y) \propto \nabla_{x_t} \log q(x_t) + \nabla_{x_t} \log q(y|x_t)$, introduced in [76, 77]. y denotes the condition and x_t defines the image at timestep t . The last term implies the conditional gradient, while the first term implies the unconditional denoiser. Complex finger articulations make the preservation of the fingers a challenging problem. As a result, we need an extra guidance from the mask. Thus, we additionally incorporate the regional mask-aware gradient guidance, proposed by [59], on the conditional gradient. Such guidance is given by,

$$\nabla_{z_t} \log q(y|x_t) = \mathbf{m}_{\text{edit}} \cdot \nabla_{x_t} \mathcal{E}_{\text{edit}} + (1 - \mathbf{m}_{\text{edit}}) \cdot \nabla_{x_t} \mathcal{E}_{\text{content}},$$

where the mask \mathbf{m}_{edit} lies in the edited region, and \mathcal{E} is the energy functions. We provide more details in the supplementary Appendix E. Moreover, we observe that it is easy to get a result that is not edited sufficiently, if we solely rely on the ODE [75], e.g., [59]. This phenomenon on grasping editing problem encouraged us to adopt the interval-timestep combination, inspired by [60], of SDE [29] and ODE [75] to involve more flexibility without harming the overall context. Then, the sampling is

as follows,

$$x_{t-1} = \begin{cases} \mathbf{m}_{\text{edit}} \cdot \mathcal{F}(x_t; \eta_1) + (1 - \mathbf{m}_{\text{edit}}) \cdot \mathcal{F}(x_t; \eta_2) & , T - t < n \text{ and } t\%2 = 0 \\ \mathcal{F}(x_t; 0) & , \text{otherwise,} \end{cases}$$

where $\eta_1 > \eta_2$. \mathcal{F} means the non-Markovian process in DDIM [75], described in Appendix E. Following Equation (11) (in supplementary), when $\eta \neq 0$, the process becomes stochastic (SDE) with the random noise involved (otherwise, ODE).

Object Replacement. GenHeld2D can also be used to replace an object in people’s hands rather than adding a new one. In this setting we perform hand segmentation [37, 97], remove the object and inpaint the background [71]. Although, SD inpainter is prone to fail when human hands are involved (Fig. 2), we find that inpainting only the object does not degrade the results. After inpainting, we perform the same pipeline as the Object Pasting process.

Non-Grasping Hand Pose Rejection. Throughout the pipeline, we assume that the input hand image shows a grasping pose – either with or without object. Previously, UGG [47] and DexGraspNet [87] suggested a method to evaluate the generated hand pose by deciding whether the hand is grasping or not. Inspired by this, to filter out the potential non-grasping hand image input, we propose a method using the ConvexHull as described in the supplementary (Appendix C).

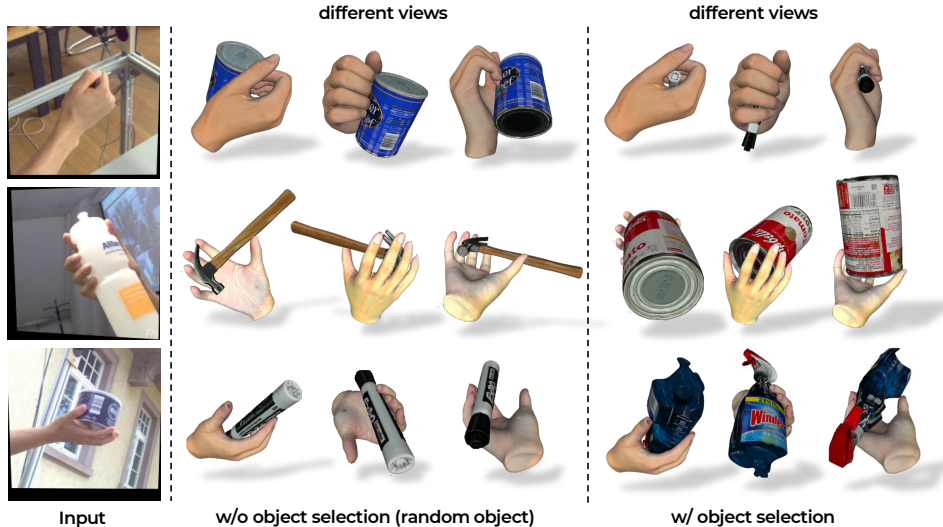


Figure 6: Ablation study of the Object Selection Network with YCB [10] objects. We observe that object selection is an important step to ensure the plausibility of generated held objects.

4 Experiments

In this section, we provide qualitative and quantitative results, and justify key design decisions. For more details, please see the Appendix.

Datasets and Setting. We trained our Object Selection Network from scratch with the DexYCB [13] dataset which consists of 582K frames with 10 real human subjects and 20 real objects with accurately known sizes. For 2D input images, we used the test images (4K) from the FreiHAND [103] dataset for overall experiments and HO3D [23] in Table 1 for fair comparison. For building the object code space, we use an existing graspable object dataset [10]. For the object fitting, we use the Adam [36] optimizer and set the max number of iterations as 4K.

	SD↓ [cm]	Pene depth↓ [cm]	Pene vox.↓ [cm ³]
GraspTTA [33]	3.21	1.05	4.58
Cpf [93]	2.77	1.14	3.46
DGrasp [16]	1.9	-	-
Ours	1.23	1.11	3.02

Table 1: Grasping quality comparison. **GenHeld3D** outperforms existing work.

4.1 GenHeld3D Results

In this section, we evaluate the grasp quality (Table 1) and object plausibility (Table 2) of GenHeld3D. For the Object Selection network, we perform an ablation study in Table 3, by using the grasping quality metrics. We also show visual results in Figure 6.

Evaluation Metrics. For the grasping quality, we employ the common metrics with the exactly same hyper-parameters with GraspTTA [33], Cpf [93], and DGrasp [16]. We used the PyBullet [22] simulator for the Simulation Distance (SD). We also compute the maximum penetrating depth and the penetrating volume of the discretized voxels that are penetrating. The average hand size was 229.947 cm^3 . For the object selection plausibility, we measure how the selected object matches the hand pose, by counting the number of object fitting steps until the loss reaches half the initial loss. At (N/A), we put the number of instances that failed to reach the halving loss until the maximum number of iterations.

	w/o selection	w/ selection
# of iters↓	3235.9 (N/A 53)	1837.3 (N/A 21)

Table 2: Object Selection plausibility. We see a significant reduction in object fitting time when the selection network is used.

	SD[cm]↓	Success ratio↑	Pene depth[cm]↓	Pene vox.[cm ³]↓
w/o selection	1.298±1.698	0.604±0.489	0.316±0.436	4.541±6.276
w/o shape code	1.341±1.884	0.690±0.433	0.312±0.530	4.003±5.239
w/o O	1.090±1.342	0.645±0.613	0.238±0.337	4.424±5.011
w/o h_c	1.203±2.015	0.432±0.587	0.180±0.509	2.908±5.219
Ours (full)	0.791±0.829	0.791±0.829	0.178±0.490	2.687±5.456

Table 3: Ablation study of the Object Selection network. Object selection, shape code, object point cloud and contacts are all essential for best performance.

Analysis. Table 1 shows the ability of our object selection and object fitting results in high quality in grasping. The ability of the Object Selection network is further demonstrated in Tab. 2. When the Object Selection network is applied, our object fitting shows a significantly faster convergence. This signifies that the predicted objects were plausible enough to ease the grasping process. The necessity of the Object Selection is also illustrated in Fig. 6. The ablation study of Object Selection network and other components is shown in Tab. 3. The w/o shape code is when we make the Object Selection network directly predict a object category and re-scale the Objaverse [19] object by its radius. Only when all the components claimed in our architecture are given, we get our best results.

4.2 GenHeld2D Results

	Imagic [35]	Pix2Pix [9]	Ours
(a) FID ↓	155.83	162.2	135.45
(b) CLIP score (prompt) ↑	0.24	0.26	0.25
(c) CLIP score "realistic" ↑	0.20	0.19	0.28
(d) masked PSNR [dB] ↑	29.055	31.875	34.002
(e) Time ↓	20m 25s	15s	1m 48s

Table 4: (a-c) Image fidelity, and (d) hand preservation of GenHeld2D

We compare the distance between the features of the FreiHAND testset images and those of our synthesized images by FID [27]. Roughly half of the FreiHAND testset images are empty hands, and the other half are hands with object. We used the second half only, when we compute the FID score. For the CLIP [70] score, we evaluated how the synthesized images align with the prompt "Hand holding an object". We assume that the relatively poor understanding of general-purpose models resulted in the minimal differences between methods in Tab. 4. Therefore, we introduce another measure, which is CLIP score on the text "realistic", to additionally evaluate the realism of the generated images. Lastly, we propose the masked PSNR. We use the ground-truth hand mask provided by FreiHAND [103] and compute the PSNR between the input and output images in the masked regions. By doing this, we try to measure the preservation of the hand in the edited images.

Analysis. We show the generated image quality in Tab. 4. Overall, our method shows a significant elevation of (a-c) the edited image fidelity and (d) the hand preservation. Fig. 8 compares the

In this section, we evaluate the GenHeld2D. In tab, 4, we compare the image quality and hand preservation in the result images. Fig. 8 shows the held object addition results. Fig. 7 demonstrates the held object replacement results.

Evaluation Metrics. First, we

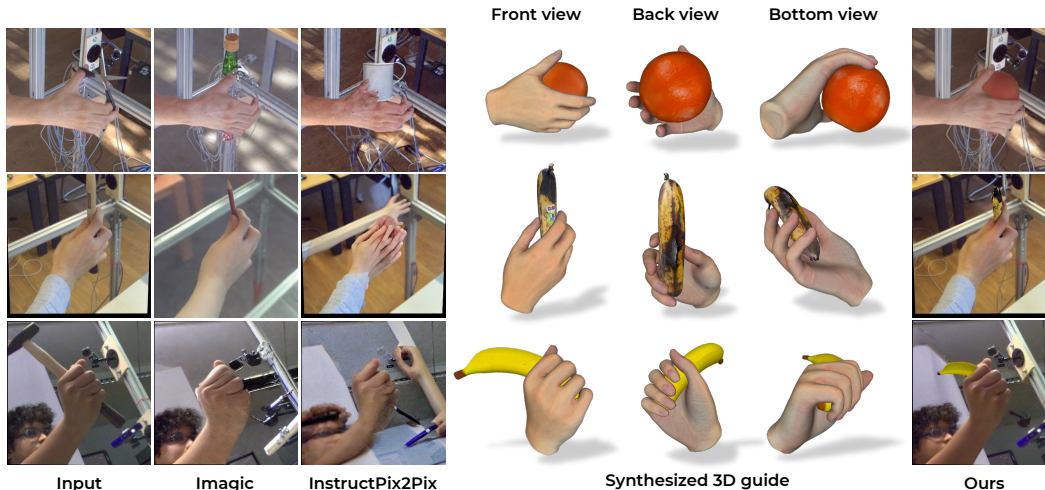


Figure 7: The object replacement application. For Imagic [35] and InstructPix2Pix [9] which can only rely on text prompts, we gave *"Replace the object in the hand with another object"*.

qualitative results between ours, Imagic [35], and InstructPix2Pix [9]. [35] and [9] both shows artifacts in fingers and often fails to make the hand holding a new object. On the other hand, with the 3D guides, we can achieve the results with higher fidelity. Finally, we showcase the Object replacement application in Fig. 7. Similar with the object generation, our paradigm of automatic category prediction and the grasping optimization in 3D significantly alleviate the artifacts and unrealistic hand-object shown in the existing methods [9, 35].

5 Conclusion

We introduced GenHeld, a method to generate handheld objects conditioned on a 3D hand model or 2D hand image. GenHeld3D operates entirely in 3D and takes as input a 3D hand model. The key insight is to estimate **object codes** that capture the space of plausible objects and can be used to select plausible and diverse objects from a large dataset. GenHeld2D takes this a step further by enabling us to edit hand images directly to either add or replace held objects.

Limitations, Future Work, and Societal Impact Although our method works well and outperforms existing methods, it is still slow and can be improved for in-the-wild images – we aim to address these limitations in future work. As a method capable of image editing, our model can be used to misrepresent objects being held by people in images. We plan to add watermarking capability to mitigate this problem.

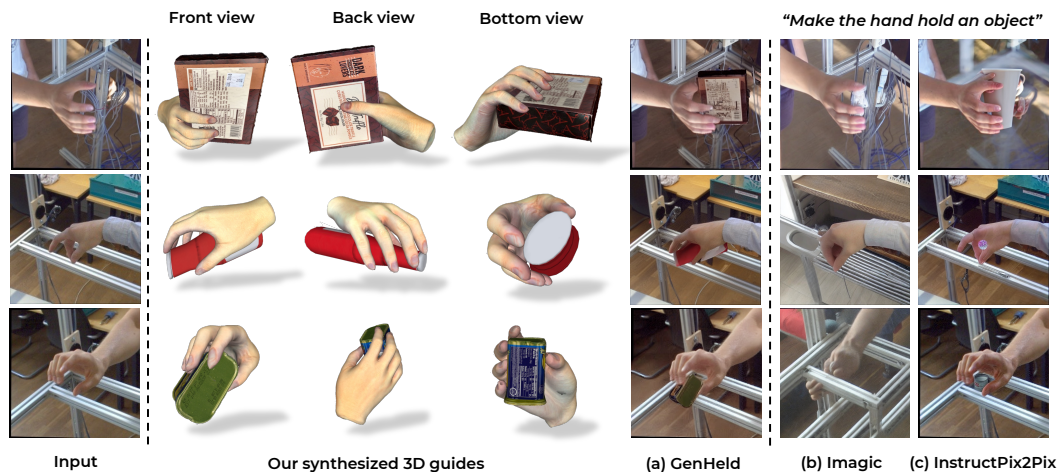


Figure 8: Qualitative comparison with the Imagic [35] and the InstructPix2Pix [9] which can only rely on text prompts.

References

- [1] Criminals wearing prosthetic fingers - twitter. <https://x.com/bristowbailey/status/1625165718340640769/>. (Accessed on 5/7/2024).
- [2] Why ai art struggles with hands - youtube. <https://www.youtube.com/watch?v=24yjRbBah3w>. (Accessed on 5/7/2024).
- [3] Hervé Abdi and Lynne J Williams. Principal component analysis. *Wiley interdisciplinary reviews: computational statistics*, 2(4):433–459, 2010.
- [4] Ferran Argelaguet and Carlos Andujar. A survey of 3d object selection techniques for virtual environments. *Computers & Graphics*, 37(3):121–136, 2013.
- [5] Fan Bao, Shen Nie, Kaiwen Xue, Chongxuan Li, Shi Pu, Yaole Wang, Gang Yue, Yue Cao, Hang Su, and Jun Zhu. One transformer fits all distributions in multi-modal diffusion at scale. In *International Conference on Machine Learning*, pages 1692–1717. PMLR, 2023.
- [6] Bharat Lal Bhatnagar, Xianghui Xie, Ilya A Petrov, Cristian Sminchisescu, Christian Theobalt, and Gerard Pons-Moll. Behave: Dataset and method for tracking human object interactions. In *Proceedings of the IEEE/CVF Conference on Computer Vision and Pattern Recognition*, pages 15935–15946, 2022.
- [7] Antonio Bicchi. On the closure properties of robotic grasping. *The International Journal of Robotics Research*, 14(4):319–334, 1995.
- [8] Samarth Brahmabhatt, Chengcheng Tang, Christopher D Twigg, Charles C Kemp, and James Hays. Contactpose: A dataset of grasps with object contact and hand pose. In *Computer Vision—ECCV 2020: 16th European Conference, Glasgow, UK, August 23–28, 2020, Proceedings, Part XIII 16*, pages 361–378. Springer, 2020.
- [9] Tim Brooks, Aleksander Holynski, and Alexei A Efros. Instructpix2pix: Learning to follow image editing instructions. In *Proceedings of the IEEE/CVF Conference on Computer Vision and Pattern Recognition*, pages 18392–18402, 2023.
- [10] Berk Calli, Arjun Singh, James Bruce, Aaron Walsman, Kurt Konolige, Siddhartha Srinivasa, Pieter Abbeel, and Aaron M Dollar. Yale-cmu-berkeley dataset for robotic manipulation research. *The International Journal of Robotics Research*, 36(3):261–268, 2017.
- [11] Angel X Chang, Thomas Funkhouser, Leonidas Guibas, Pat Hanrahan, Qixing Huang, Zimo Li, Silvio Savarese, Manolis Savva, Shuran Song, Hao Su, et al. Shapenet: An information-rich 3d model repository. *arXiv preprint arXiv:1512.03012*, 2015.
- [12] Xiaoyun Chang and Yi Sun. Text2grasp: Grasp synthesis by text prompts of object grasping parts. *arXiv preprint arXiv:2404.15189*, 2024.
- [13] Yu-Wei Chao, Wei Yang, Yu Xiang, Pavlo Molchanov, Ankur Handa, Jonathan Tremblay, Yashraj S Narang, Karl Van Wyk, Umar Iqbal, Stan Birchfield, et al. Dexycb: A benchmark for capturing hand grasping of objects. In *Proceedings of the IEEE/CVF Conference on Computer Vision and Pattern Recognition*, pages 9044–9053, 2021.
- [14] Xiangyu Chen, Xintao Wang, Jiantao Zhou, Yu Qiao, and Chao Dong. Activating more pixels in image super-resolution transformer. In *Proceedings of the IEEE/CVF conference on computer vision and pattern recognition*, pages 22367–22377, 2023.
- [15] Yujin Chen, Zhigang Tu, Di Kang, Linchao Bao, Ying Zhang, Xuefei Zhe, Ruizhi Chen, and Junsong Yuan. Model-based 3d hand reconstruction via self-supervised learning. In *Proceedings of the IEEE/CVF Conference on Computer Vision and Pattern Recognition*, pages 10451–10460, 2021.
- [16] Sammy Christen, Muhammed Kocabas, Emre Aksan, Jemin Hwangbo, Jie Song, and Otmar Hilliges. D-grasp: Physically plausible dynamic grasp synthesis for hand-object interactions. In *Proceedings of the IEEE/CVF Conference on Computer Vision and Pattern Recognition*, pages 20577–20586, 2022.

- [17] Sammy Christen, Shreyas Hampali, Fadime Sener, Edoardo Remelli, Tomas Hodan, Eric Sauser, Shugao Ma, and Bugra Tekin. Diffh2o: Diffusion-based synthesis of hand-object interactions from textual descriptions. *arXiv preprint arXiv:2403.17827*, 2024.
- [18] Hongkai Dai, Anirudha Majumdar, and Russ Tedrake. Synthesis and optimization of force closure grasps via sequential semidefinite programming. *Robotics Research: Volume 1*, pages 285–305, 2018.
- [19] Matt Deitke, Dustin Schwenk, Jordi Salvador, Luca Weihs, Oscar Michel, Eli VanderBilt, Ludwig Schmidt, Kiana Ehsani, Aniruddha Kembhavi, and Ali Farhadi. Objaverse: A universe of annotated 3d objects. In *Proceedings of the IEEE/CVF Conference on Computer Vision and Pattern Recognition*, pages 13142–13153, 2023.
- [20] Zicong Fan, Omid Taheri, Dimitrios Tzionas, Muhammed Kocabas, Manuel Kaufmann, Michael J Black, and Otmar Hilliges. Arctic: A dataset for dexterous bimanual hand-object manipulation. In *Proceedings of the IEEE/CVF Conference on Computer Vision and Pattern Recognition*, pages 12943–12954, 2023.
- [21] Mohit Goyal, Sahil Modi, Rishabh Goyal, and Saurabh Gupta. Human hands as probes for interactive object understanding. In *Proceedings of the IEEE/CVF Conference on Computer Vision and Pattern Recognition*, pages 3293–3303, 2022.
- [22] Klaus Greff, Francois Belletti, Lucas Beyer, Carl Doersch, Yilun Du, Daniel Duckworth, David J Fleet, Dan Gnanapragasam, Florian Golemo, Charles Herrmann, et al. Kubric: A scalable dataset generator. In *Proceedings of the IEEE/CVF conference on computer vision and pattern recognition*, pages 3749–3761, 2022.
- [23] Shreyas Hampali, Sayan Deb Sarkar, Mahdi Rad, and Vincent Lepetit. Keypoint transformer: Solving joint identification in challenging hands and object interactions for accurate 3d pose estimation. In *Proceedings of the IEEE/CVF Conference on Computer Vision and Pattern Recognition*, pages 11090–11100, 2022.
- [24] Yana Hasson, Gul Varol, Dimitrios Tzionas, Igor Kalevatykh, Michael J Black, Ivan Laptev, and Cordelia Schmid. Learning joint reconstruction of hands and manipulated objects. In *Proceedings of the IEEE/CVF conference on computer vision and pattern recognition*, pages 11807–11816, 2019.
- [25] Kaiming He, Xiangyu Zhang, Shaoqing Ren, and Jian Sun. Deep residual learning for image recognition. In *Proceedings of the IEEE conference on computer vision and pattern recognition*, pages 770–778, 2016.
- [26] Amir Hertz, Ron Mokady, Jay Tenenbaum, Kfir Aberman, Yael Pritch, and Daniel Cohen-Or. Prompt-to-prompt image editing with cross attention control, 2022.
- [27] Martin Heusel, Hubert Ramsauer, Thomas Unterthiner, Bernhard Nessler, and Sepp Hochreiter. Gans trained by a two time-scale update rule converge to a local nash equilibrium. *Advances in neural information processing systems*, 30, 2017.
- [28] Jonathan Ho and Tim Salimans. Classifier-free diffusion guidance. *arXiv preprint arXiv:2207.12598*, 2022.
- [29] Jonathan Ho, Ajay Jain, and Pieter Abbeel. Denoising diffusion probabilistic models. *Advances in neural information processing systems*, 33:6840–6851, 2020.
- [30] W Stamps Howard and Vijay Kumar. On the stability of grasped objects. *IEEE transactions on robotics and automation*, 12(6):904–917, 1996.
- [31] Kirk Huslage, William A Rutala, Emily Sickbert-Bennett, and David J Weber. A quantitative approach to defining “high-touch” surfaces in hospitals. *Infection Control & Hospital Epidemiology*, 31(8):850–853, 2010.
- [32] Juntao Jian, Xiuping Liu, Manyi Li, Ruizhen Hu, and Jian Liu. Affordpose: A large-scale dataset of hand-object interactions with affordance-driven hand pose. In *Proceedings of the IEEE/CVF International Conference on Computer Vision*, pages 14713–14724, 2023.

- [33] Hanwen Jiang, Shaowei Liu, Jiashun Wang, and Xiaolong Wang. Hand-object contact consistency reasoning for human grasps generation. In *Proceedings of the IEEE/CVF international conference on computer vision*, pages 11107–11116, 2021.
- [34] Korrawe Karunratanakul, Jinlong Yang, Yan Zhang, Michael J Black, Krikamol Muandet, and Siyu Tang. Grasping field: Learning implicit representations for human grasps. In *2020 International Conference on 3D Vision (3DV)*, pages 333–344. IEEE, 2020.
- [35] Bahjat Kawar, Shiran Zada, Oran Lang, Omer Tov, Huiwen Chang, Tali Dekel, Inbar Mosseri, and Michal Irani. Imagic: Text-based real image editing with diffusion models. In *Proceedings of the IEEE/CVF Conference on Computer Vision and Pattern Recognition*, pages 6007–6017, 2023.
- [36] Diederik P Kingma and Jimmy Ba. Adam: A method for stochastic optimization. *arXiv preprint arXiv:1412.6980*, 2014.
- [37] Alexander Kirillov, Eric Mintun, Nikhila Ravi, Hanzi Mao, Chloe Rolland, Laura Gustafson, Tete Xiao, Spencer Whitehead, Alexander C Berg, Wan-Yen Lo, et al. Segment anything. In *Proceedings of the IEEE/CVF International Conference on Computer Vision*, pages 4015–4026, 2023.
- [38] Arjun Sriram Lakshmipathy, Nicole Feng, Yu Xi Lee, Moshe Mahler, and Nancy Pollard. Contact edit: Artist tools for intuitive modeling of hand-object interactions. *ACM Transactions on Graphics (TOG)*, 42(4):1–20, 2023.
- [39] Kailin Li, Jingbo Wang, Lixin Yang, Cewu Lu, and Bo Dai. Semgrasp: Semantic grasp generation via language aligned discretization. *arXiv preprint arXiv:2404.03590*, 2024.
- [40] Puhao Li, Tengyu Liu, Yuyang Li, Yiran Geng, Yixin Zhu, Yaodong Yang, and Siyuan Huang. Gendexgrasp: Generalizable dexterous grasping. In *2023 IEEE International Conference on Robotics and Automation (ICRA)*, pages 8068–8074. IEEE, 2023.
- [41] Yuwei Li, Longwen Zhang, Zesong Qiu, Yingwenqi Jiang, Nianyi Li, Yuexin Ma, Yuyao Zhang, Lan Xu, and Jingyi Yu. Nimble: a non-rigid hand model with bones and muscles. *ACM Transactions on Graphics (TOG)*, 41(4):1–16, 2022.
- [42] Jacky Liang, Viktor Makoviychuk, Ankur Handa, Nuttapong Chentanez, Miles Macklin, and Dieter Fox. Gpu-accelerated robotic simulation for distributed reinforcement learning. In *Conference on Robot Learning*, pages 270–282. PMLR, 2018.
- [43] Min Liu, Zherong Pan, Kai Xu, Kanishka Ganguly, and Dinesh Manocha. Deep differentiable grasp planner for high-dof grippers. *arXiv preprint arXiv:2002.01530*, 2020.
- [44] Shaowei Liu, Yang Zhou, Jimei Yang, Saurabh Gupta, and Shenlong Wang. Contactgen: Generative contact modeling for grasp generation. In *Proceedings of the IEEE/CVF International Conference on Computer Vision*, pages 20609–20620, 2023.
- [45] Tengyu Liu, Zeyu Liu, Ziyuan Jiao, Yixin Zhu, and Song-Chun Zhu. Synthesizing diverse and physically stable grasps with arbitrary hand structures using differentiable force closure estimator. *IEEE Robotics and Automation Letters*, 7(1):470–477, 2021.
- [46] Yumeng Liu, Yaxun Yang, Youzhuo Wang, Xiaofei Wu, Jiamin Wang, Yichen Yao, Sören Schwertfeger, Sibe Yang, Wenping Wang, Jingyi Yu, et al. Realdex: Towards human-like grasping for robotic dexterous hand. *arXiv preprint arXiv:2402.13853*, 2024.
- [47] Jiaxin Lu, Hao Kang, Haoxiang Li, Bo Liu, Yiding Yang, Qixing Huang, and Gang Hua. Ugg: Unified generative grasping. *arXiv preprint arXiv:2311.16917*, 2023.
- [48] James Lucas, George Tucker, Roger Grosse, and Mohammad Norouzi. Understanding posterior collapse in generative latent variable models. 2019.
- [49] Camillo Lugaresi, Jiuqiang Tang, Hadon Nash, Chris McClanahan, Esha Uboweja, Michael Hays, Fan Zhang, Chuo-Ling Chang, Ming Guang Yong, Juhyun Lee, et al. Mediapipe: A framework for building perception pipelines. *arXiv preprint arXiv:1906.08172*, 2019.

- [50] Priyanka Mandikal and Kristen Grauman. Dexvip: Learning dexterous grasping with human hand pose priors from video. In *Conference on Robot Learning*, pages 651–661. PMLR, 2022.
- [51] Daniel Mendes, Fabio Marco Caputo, Andrea Giachetti, Alfredo Ferreira, and Joaquim Jorge. A survey on 3d virtual object manipulation: From the desktop to immersive virtual environments. In *Computer graphics forum*, pages 21–45. Wiley Online Library, 2019.
- [52] Chenlin Meng, Yutong He, Yang Song, Jiaming Song, Jiajun Wu, Jun-Yan Zhu, and Stefano Ermon. Sdedit: Guided image synthesis and editing with stochastic differential equations. *arXiv preprint arXiv:2108.01073*, 2021.
- [53] Ben Mildenhall, Pratul P Srinivasan, Matthew Tancik, Jonathan T Barron, Ravi Ramamoorthi, and Ren Ng. Nerf: Representing scenes as neural radiance fields for view synthesis. *Communications of the ACM*, 65(1):99–106, 2021.
- [54] Andrew T Miller and Peter K Allen. Graspit! a versatile simulator for robotic grasping. *IEEE Robotics & Automation Magazine*, 11(4):110–122, 2004.
- [55] Kaichun Mo, Shilin Zhu, Angel X Chang, Li Yi, Subarna Tripathi, Leonidas J Guibas, and Hao Su. Partnet: A large-scale benchmark for fine-grained and hierarchical part-level 3d object understanding. In *Proceedings of the IEEE/CVF conference on computer vision and pattern recognition*, pages 909–918, 2019.
- [56] Kaichun Mo, Leonidas J Guibas, Mustafa Mukadam, Abhinav Gupta, and Shubham Tulsiani. Where2act: From pixels to actions for articulated 3d objects. In *Proceedings of the IEEE/CVF International Conference on Computer Vision*, pages 6813–6823, 2021.
- [57] Tomas Möller and Ben Trumbore. Fast, minimum storage ray/triangle intersection. In *ACM SIGGRAPH 2005 Courses*, pages 7–es. 2005.
- [58] David J Montana. The condition for contact grasp stability. In *ICRA*, pages 412–417, 1991.
- [59] Chong Mou, Xintao Wang, Jiechong Song, Ying Shan, and Jian Zhang. Dragondiffusion: Enabling drag-style manipulation on diffusion models. *arXiv preprint arXiv:2307.02421*, 2023.
- [60] Chong Mou, Xintao Wang, Jiechong Song, Ying Shan, and Jian Zhang. Diffeditor: Boosting accuracy and flexibility on diffusion-based image editing. *arXiv preprint arXiv:2402.02583*, 2024.
- [61] Jiteng Mu, Michaël Gharbi, Richard Zhang, Eli Shechtman, Nuno Vasconcelos, Xiaolong Wang, and Taesung Park. Editable image elements for controllable synthesis. *arXiv preprint arXiv:2404.16029*, 2024.
- [62] Supreeth Narasimhaswamy, Uttaran Bhattacharya, Xiang Chen, Ishita Dasgupta, Saayan Mitra, and Minh Hoai. Handdiffuser: Text-to-image generation with realistic hand appearances, 2024.
- [63] Rhys Newbury, Morris Gu, Lachlan Chumbley, Arsalan Mousavian, Clemens Eppner, Jürgen Leitner, Jeannette Bohg, Antonio Morales, Tamim Asfour, Danica Kragic, et al. Deep learning approaches to grasp synthesis: A review. *IEEE Transactions on Robotics*, 2023.
- [64] Karran Pandey, Paul Guerrero, Matheus Gadelha, Yannick Hold-Geoffroy, Karan Singh, and Niloy Mitra. Diffusion handles: Enabling 3d edits for diffusion models by lifting activations to 3d. *arXiv preprint arXiv:2312.02190*, 2023.
- [65] Patrick Pérez, Michel Gangnet, and Andrew Blake. Poisson image editing. In *Seminal Graphics Papers: Pushing the Boundaries, Volume 2*, pages 577–582. 2023.
- [66] Ilya A Petrov, Riccardo Marin, Julian Chibane, and Gerard Pons-Moll. Object pop-up: Can we infer 3d objects and their poses from human interactions alone? In *Proceedings of the IEEE/CVF Conference on Computer Vision and Pattern Recognition*, pages 4726–4736, 2023.
- [67] Charles R Qi, Hao Su, Kaichun Mo, and Leonidas J Guibas. Pointnet: Deep learning on point sets for 3d classification and segmentation. In *Proceedings of the IEEE conference on computer vision and pattern recognition*, pages 652–660, 2017.

- [68] Charles Ruizhongtai Qi, Li Yi, Hao Su, and Leonidas J Guibas. Pointnet++: Deep hierarchical feature learning on point sets in a metric space. *Advances in neural information processing systems*, 30, 2017.
- [69] Neng Qian, Jiayi Wang, Franziska Mueller, Florian Bernard, Vladislav Golyanik, and Christian Theobalt. Html: A parametric hand texture model for 3d hand reconstruction and personalization. In *Computer Vision–ECCV 2020: 16th European Conference, Glasgow, UK, August 23–28, 2020, Proceedings, Part XI 16*, pages 54–71. Springer, 2020.
- [70] Alec Radford, Jong Wook Kim, Chris Hallacy, Aditya Ramesh, Gabriel Goh, Sandhini Agarwal, Girish Sastry, Amanda Askell, Pamela Mishkin, Jack Clark, et al. Learning transferable visual models from natural language supervision. In *International conference on machine learning*, pages 8748–8763. PMLR, 2021.
- [71] Robin Rombach, Andreas Blattmann, Dominik Lorenz, Patrick Esser, and Björn Ommer. High-resolution image synthesis with latent diffusion models. In *Proceedings of the IEEE/CVF conference on computer vision and pattern recognition*, pages 10684–10695, 2022.
- [72] Javier Romero, Dimitrios Tzionas, and Michael J Black. Embodied hands: Modeling and capturing hands and bodies together. *arXiv preprint arXiv:2201.02610*, 2022.
- [73] Rahul Sajnani, Jeroen Vanbaar, Jie Min, Kapil Katyal, and Srinath Sridhar. Geodiffuser: Geometry-based image editing with diffusion models. *arXiv preprint arXiv:2404.14403*, 2024.
- [74] Qijin She, Shishun Zhang, Yunfan Ye, Min Liu, Ruizhen Hu, and Kai Xu. Learning cross-hand policies for high-dof reaching and grasping. *arXiv preprint arXiv:2404.09150*, 2024.
- [75] Jiaming Song, Chenlin Meng, and Stefano Ermon. Denoising diffusion implicit models. *arXiv preprint arXiv:2010.02502*, 2020.
- [76] Yang Song and Stefano Ermon. Improved techniques for training score-based generative models. *Advances in neural information processing systems*, 33:12438–12448, 2020.
- [77] Yang Song, Jascha Sohl-Dickstein, Diederik P Kingma, Abhishek Kumar, Stefano Ermon, and Ben Poole. Score-based generative modeling through stochastic differential equations. *arXiv preprint arXiv:2011.13456*, 2020.
- [78] Omid Taheri, Nima Ghorbani, Michael J Black, and Dimitrios Tzionas. Grab: A dataset of whole-body human grasping of objects. In *Computer Vision–ECCV 2020: 16th European Conference, Glasgow, UK, August 23–28, 2020, Proceedings, Part IV 16*, pages 581–600. Springer, 2020.
- [79] Omid Taheri, Vasileios Choutas, Michael J Black, and Dimitrios Tzionas. Goal: Generating 4d whole-body motion for hand-object grasping. In *Proceedings of the IEEE/CVF Conference on Computer Vision and Pattern Recognition*, pages 13263–13273, 2022.
- [80] Omid Taheri, Yi Zhou, Dimitrios Tzionas, Yang Zhou, Duygu Ceylan, Soren Pirk, and Michael J Black. Grip: Generating interaction poses using spatial cues and latent consistency. In *International conference on 3D vision (3DV)*, 2024.
- [81] Jeffrey C Trinkle. On the stability and instantaneous velocity of grasped frictionless objects. *IEEE Transactions on Robotics and Automation*, 8(5):560–572, 1992.
- [82] Dylan Turpin, Liquan Wang, Eric Heiden, Yun-Chun Chen, Miles Macklin, Stavros Tsogkas, Sven Dickinson, and Animesh Garg. Grasp’d: Differentiable contact-rich grasp synthesis for multi-fingered hands. In *European Conference on Computer Vision*, pages 201–221. Springer, 2022.
- [83] Julen Urain, Niklas Funk, Jan Peters, and Georgia Chalvatzaki. Se (3)-diffusionfields: Learning smooth cost functions for joint grasp and motion optimization through diffusion. In *2023 IEEE International Conference on Robotics and Automation (ICRA)*, pages 5923–5930. IEEE, 2023.
- [84] Ashish Vaswani, Noam Shazeer, Niki Parmar, Jakob Uszkoreit, Llion Jones, Aidan N Gomez, Łukasz Kaiser, and Illia Polosukhin. Attention is all you need. *Advances in neural information processing systems*, 30, 2017.

- [85] Bruce A Wallace. Merging and transformation of raster images for cartoon animation. In *Proceedings of the 8th annual conference on Computer graphics and interactive techniques*, pages 253–262, 1981.
- [86] Weikang Wan, Haoran Geng, Yun Liu, Zikang Shan, Yaodong Yang, Li Yi, and He Wang. Unidexgrasp++: Improving dexterous grasping policy learning via geometry-aware curriculum and iterative generalist-specialist learning. In *Proceedings of the IEEE/CVF International Conference on Computer Vision*, pages 3891–3902, 2023.
- [87] Ruicheng Wang, Jialiang Zhang, Jiayi Chen, Yinzheng Xu, Puhao Li, Tengyu Liu, and He Wang. Dexgraspnet: A large-scale robotic dexterous grasp dataset for general objects based on simulation. In *2023 IEEE International Conference on Robotics and Automation (ICRA)*, pages 11359–11366. IEEE, 2023.
- [88] Zehang Weng, Haofei Lu, Danica Kragic, and Jens Lundell. Dexdiffuser: Generating dexterous grasps with diffusion models. *arXiv preprint arXiv:2402.02989*, 2024.
- [89] Robert L Whitwell and Melvyn A Goodale. Grasping without vision: time normalizing grip aperture profiles yields spurious grip scaling to target size. *Neuropsychologia*, 51(10): 1878–1887, 2013.
- [90] Robert L Whitwell, A David Milner, and Melvyn A Goodale. The two visual systems hypothesis: new challenges and insights from visual form agnostic patient df. *Frontiers in neurology*, 5:119156, 2014.
- [91] Yan Wu, Jiahao Wang, Yan Zhang, Siwei Zhang, Otmar Hilliges, Fisher Yu, and Siyu Tang. Saga: Stochastic whole-body grasping with contact. In *European Conference on Computer Vision*, pages 257–274. Springer, 2022.
- [92] Binxin Yang, Shuyang Gu, Bo Zhang, Ting Zhang, Xuejin Chen, Xiaoyan Sun, Dong Chen, and Fang Wen. Paint by example: Exemplar-based image editing with diffusion models. In *Proceedings of the IEEE/CVF Conference on Computer Vision and Pattern Recognition*, pages 18381–18391, 2023.
- [93] Lixin Yang, Xinyu Zhan, Kailin Li, Wenqiang Xu, Jiefeng Li, and Cewu Lu. Cpf: Learning a contact potential field to model the hand-object interaction. In *Proceedings of the IEEE/CVF International Conference on Computer Vision*, pages 11097–11106, 2021.
- [94] Yufei Ye, Xueting Li, Abhinav Gupta, Shalini De Mello, Stan Birchfield, Jiaming Song, Shubham Tulsiani, and Sifei Liu. Affordance diffusion: Synthesizing hand-object interactions. In *Proceedings of the IEEE/CVF Conference on Computer Vision and Pattern Recognition*, pages 22479–22489, 2023.
- [95] Yufei Ye, Abhinav Gupta, Kris Kitani, and Shubham Tulsiani. G-hop: Generative hand-object prior for interaction reconstruction and grasp synthesis. *arXiv preprint arXiv:2404.12383*, 2024.
- [96] Hui Zhang, Sammy Christen, Zicong Fan, Otmar Hilliges, and Jie Song. Grasppl: Generating grasping motions for diverse objects at scale. *arXiv preprint arXiv:2403.19649*, 2024.
- [97] Lingzhi Zhang, Shenghao Zhou, Simon Stent, and Jianbo Shi. Fine-grained egocentric hand-object segmentation: Dataset, model, and applications. In *European Conference on Computer Vision*, pages 127–145. Springer, 2022.
- [98] Mengqi Zhang, Yang Fu, Zheng Ding, Sifei Liu, Zhuowen Tu, and Xiaolong Wang. Hoidiffusion: Generating realistic 3d hand-object interaction data. *arXiv preprint arXiv:2403.12011*, 2024.
- [99] Yan Zhang, Michael J Black, and Siyu Tang. We are more than our joints: Predicting how 3d bodies move. In *Proceedings of the IEEE/CVF Conference on Computer Vision and Pattern Recognition*, pages 3372–3382, 2021.

- [100] Juntian Zheng, Qingyuan Zheng, Lixing Fang, Yun Liu, and Li Yi. Cams: Canonicalized manipulation spaces for category-level functional hand-object manipulation synthesis. In *Proceedings of the IEEE/CVF Conference on Computer Vision and Pattern Recognition*, pages 585–594, 2023.
- [101] Keyang Zhou, Bharat Lal Bhatnagar, Jan Eric Lenssen, and Gerard Pons-Moll. Toch: Spatio-temporal object-to-hand correspondence for motion refinement. In *European Conference on Computer Vision*, pages 1–19. Springer, 2022.
- [102] Jiayin Zhu, Zhuoran Zhao, Linlin Yang, and Angela Yao. Hifhr: Enhancing 3d hand reconstruction from a single image via high-fidelity texture. In *DAGM German Conference on Pattern Recognition*, pages 115–130. Springer, 2023.
- [103] Christian Zimmermann, Duygu Ceylan, Jimei Yang, Bryan Russell, Max Argus, and Thomas Brox. Freihand: A dataset for markerless capture of hand pose and shape from single rgb images. In *Proceedings of the IEEE/CVF International Conference on Computer Vision*, pages 813–822, 2019.
- [104] Paula Zuccotti. *Everything we touch: A 24-hour inventory of our lives*. National Geographic Books, 2015.

A Additional Comparisons



Figure 9: Additional comparisons of Fig. 1. Even with giving the object category as text prompts, the results are inferior to the results using the 3D grasping guide. Left to right: power drill, spam can, screwdriver, bowl.

In fig. 9, (b) For [9, 35], even if we give our selected object to the text prompt, the object addition/replacement on hands fail, without our 3D guide. (c) Without knowing which object to grasp, the image editing models struggles to follow the prompt.



Figure 10: One hand pose can have multiple true answers. We sample different random noise z to get multiple answers.

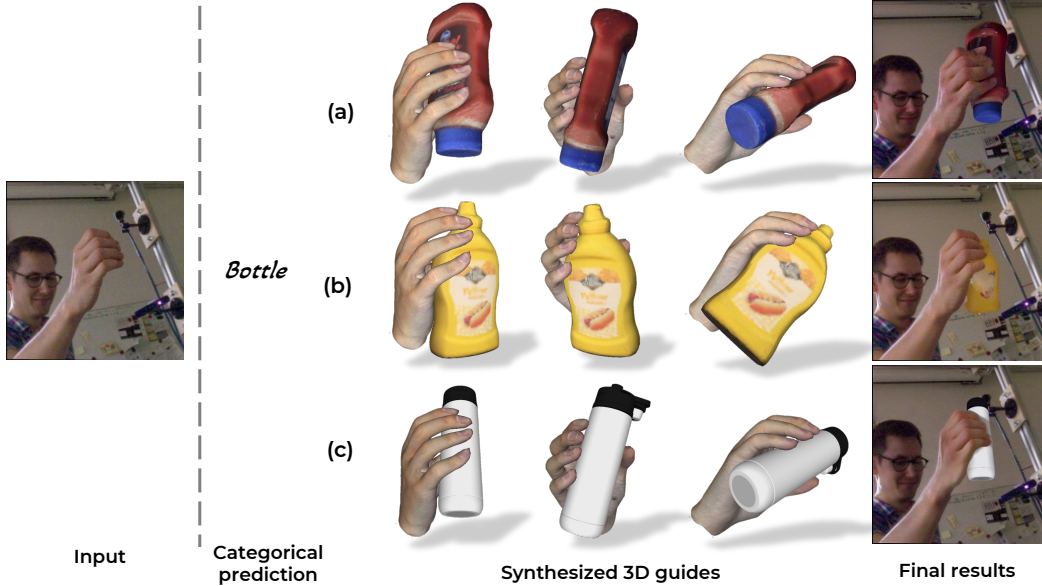


Figure 11: One categorical prediction produces different objects.

B Detailed Model Architecture

The red line shows the information that is available at inference. P.E. means Positional Encoding [53, 84] and the Object Feat and Hand Feat were obtained by the vertex normals. We incorporate PointNet [67] to encode the hand vertices. Unlike hand vertices, the number of object vertices varies depending on objects. Therefore, we leverage the global max pooling of PointNet++ [68] to encode the object vertices. For the hand mesh in the contact estimation, we use the canonicalized hand mesh, which is rotation normalized and centered around the world origin. Then, only the hand pose and shape remains for predicting the contact. By doing this, we make the prediction easier for the model. The ContactNet is inspired by GraspTTA [33]. However, it has differences in that our ContactNet only accepts the hand as a input. Following the GraspTTA, we use the architecture of CNNs with residual connections [25]. This ContactNet is separately trained in a supervised manner by DexYCB [13]. The predicted contact probability for hand vertices are converted into the xyz contact positions (Contact XYZ). Then, the Contact XYZ and the Postional Encoded [53, 84] are concatenated to the object encoder. Together with the Object Feature, these information is fed into the PointNet++ [68] encoder to make the Point Latent. The Shape Code latent comes from the Shape Code encoder. The Shape Code encoder consists of CNN with residual connections [25], following the human model model, SAGA [91]. The Shape Code latent and Point latent are entangled using the cross attention and the following Fusion Block of linear layers. Finally, the shape code is generated using the decoder. The decoder is made up of the Shape Code decoder and the Object decoder, which follows the detail with [91]. The total number of layers sums up to 102 by end-to-end.

C Non-Grasping Hand Rejection

In case the user gives an input image that does not contain the hand, the hand pose estimator and reconstructor can detect the existence of hands. However, without a non-grasping hand rejection algorithm, the model will automatically try to make an object to be grasped by that hand. For example, we should reject a rest pose hand and some of the hand gestures, e.g., thumbs-up and making "two" with hands. As a result, we propose a novel method to discriminate the grasping pose and the non-grasping pose. We illustrate this algorithm in Fig. 15 Inversely using the grasp quality evaluation metrics from UGG [47] and DexGraspNet [87], we leverage the convex hull of the reconstructed hand mesh and their maximum inscribed ball. First, we compute the Convex Hull. Then, we obtain the inscribed ball, by minimizing a loss function, given by,

$$\mathcal{L}_{\text{ins_ball}}(o) = \text{SDF}(H, o) + \text{scale}(H), \quad (5)$$



Figure 12: More 3D results. Our Object Shape code allows searching diverse plausible objects from Objaverse [19] that matches the hand input.



Figure 13: Our Object Shape code can also work with the YCB [10] objects.

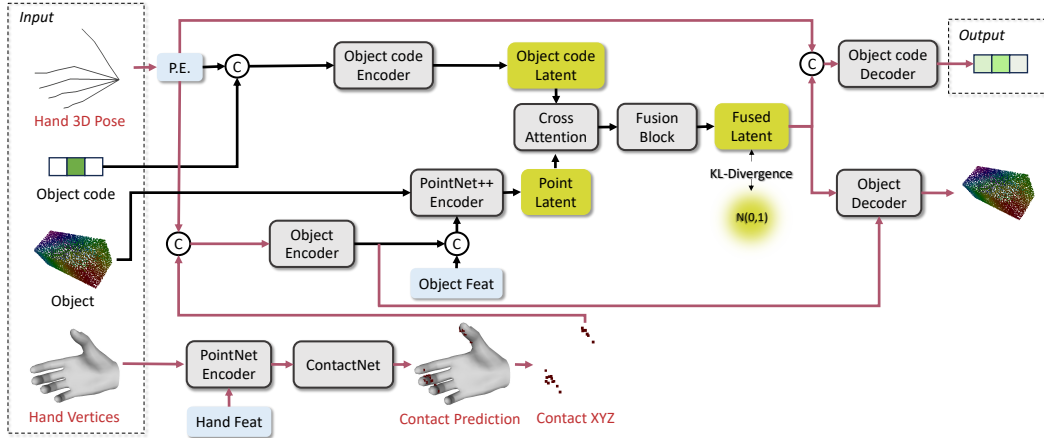


Figure 14: Details of the Object Selection network.

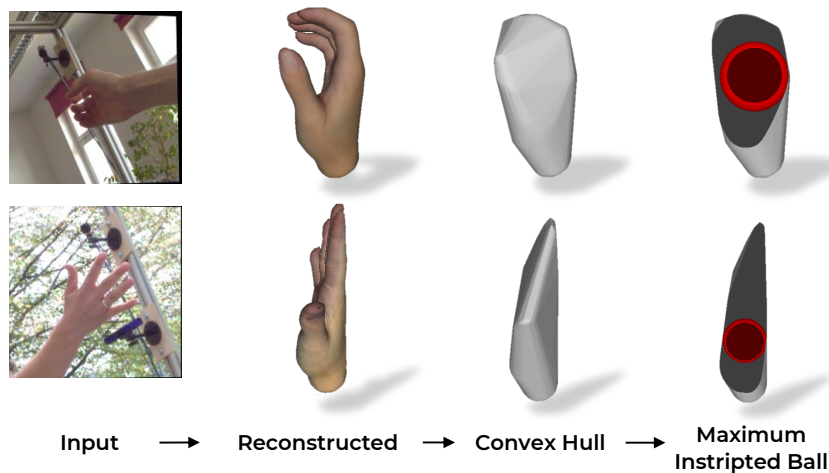


Figure 15: Non-grasping hand pose rejection algorithm (Sec. C). If the radius of maximum the inscribed ball is below a threshold, we reject that hand pose.

where the SDF takes the outside to be positive values. o means the center of the inscribed ball, and the H means the Convex Hull. $SDF(X, x)$ means the signed distance function from a point x to the mesh X . We added the scale of the Convex Hull to avoid the loss function to be negative. Then, the radius of the inscribed ball follows, $\mathcal{L}_{ins_ball}(o) - scale(H)$. Even though the convex hull of a rest pose with the fingers all separate with each other (2nd row of Fig. 15 has similar size with the grasping pose (1st row of Fig. 15, the radius of maximum inscribed ball of the Convex Hull has a strict difference. This is because the maximum inscribed ball measures the thinnest part of the hand Convex Hull. As a result, we threshold the radius of the maximum inscribed ball to discriminate the non-grasping hand. If the radius is determined to be lower than 0.4 in the normalized hand space, we simply reject such input and ask for another input.

D Simulation Loss

The ablation of the Simulation loss we incorporate in Sec. 3.1 is illustrated in Fig. 16. Note that our results on the left column still achieves almost perfect contacts and no penetration. However, these grasplings are imperfect, because the hands are not grasping the object with high physical stability. Therefore, we add extra constraints to the Eq. 4, i.e., Eq. 6. Following [45], we ensure the force exerted to the object is "closed" by multiple direction, so that the object will stay still by the frictions of the hand and the object. Let us denote the contact points during optimization as $g_i, i = \{1, 2, \dots, N\}$, where N is the number of contact points. For the friction cone axes, we compute

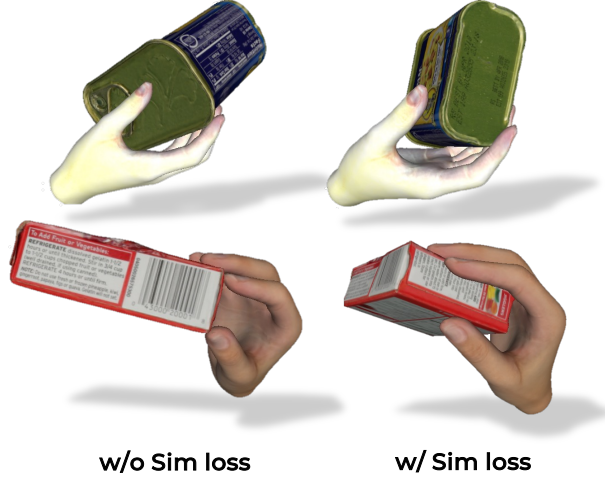


Figure 16: Ablation study of the Sim loss (Eq. 6).

the surface normals \hat{n}_i from the contact vertices. Then, following the force closure [18] constraints,

$$\mathcal{L}_{\text{sim}} = \text{eigen}_0(GG' - \epsilon I) + \|G\hat{n}\|_2 + \lambda_{\text{dist}} \sum_{g_i \in g} d(g_i, V_{\text{obj}}) \quad (6)$$

should be minimized, where

$$G = \begin{bmatrix} I_{3 \times 3} & I_{3 \times 3} & \dots & I_{3 \times 3} \\ [g_1]_{\times} & [g_2]_{\times} & \dots & [g_N]_{\times} \end{bmatrix}, \quad (7)$$

and $[\cdot]_{\times}$ denotes skew-symmetric matrix. eigen_0 is the smallest Eigenvalue.

Below, we further justify the Eq. 6 and the use of Eq. 7. When the G matrix is given by Eq. 7 with the contact points $g_i, i = \{1, 2, \dots, N\}$, [18] introduced the constraints to satisfy the contact forces to make a closure as follows,

$$\begin{aligned} GG' &\succcurlyeq \epsilon I_{6 \times 6}, \\ Gf &= 0, \\ f_i^T e_i &> \frac{1}{\sqrt{\mu^2 + 1}} |f_i|, \\ g_i &\in S_i, \end{aligned} \quad (8)$$

where S is the object surface and the f_i is the contact forces at the contact points g_i and e_i defines the friction cone axis. μ_i is the friction cone coefficient. N denotes the number of contact points. We find that the derivation from [45] can effectively lead these constraints into Eq. 6 by decomposing the f into the normal component f_n and the tangential component f_t . Then, the second line of Eq. 8 can be rewritten by,

$$\begin{aligned} Gf &= f(f_n + f_t) = 0, \\ G \frac{f_n}{\|f_n\|_2} &= - \frac{Gf_t}{\|f_n\|_2}, \\ Gc &= - \frac{Gf_t}{\|f_n\|_2}, \end{aligned} \quad (9)$$

which automatically lead to the rewritten formulation of the second line of Eq. 8 as follows,

$$\|Gc\|_2 < \delta \quad (10)$$

, where δ is a small number. We exploit the vertex normal of the contact points as the friction cone axis e_i . In conclusion, following the first and last line of Eq. 8 and the Eq. 10, we can easily reach the conclusion that the force closure is achieved by minimizing the loss presented in the Eq. 6.

E 2D Image Editing

In this section, we provide the missing details of Eq. 5 and 5. Following the DDIM [75] non-Markovian process, one can generate x_{t-1} from s_t as,

$$x_{t-1} = \sqrt{\alpha_{t-1}} \left(\frac{x_t - \sqrt{1 - \alpha_t} \epsilon_\theta^{(t)}(x_t)}{\sqrt{\alpha_t}} \right) + \sqrt{1 - \alpha_{t-1} - \sigma_t^2} \cdot \epsilon_\theta^{(t)}(x_t) + \sigma_t \epsilon_t, \quad (11)$$

where $\sigma_t = \eta \sqrt{(1 - \alpha_{t-1}) / (1 - \alpha_t)} \sqrt{1 - \alpha_t / \alpha_{t-1}}$. The first term means the predicted x_0 , and the second term indicates the direction pointing to x_t . The last term is the random noise. Affected by [60], we control the last term, i.e., the random noise, by introducing η to the σ_t . With $\eta = 0$, Eq. 11 loses its randomness and becomes deterministic. We use this for Eq. 5 to balance between the stochastic process and the deterministic process.

Inspired by [59], the energy functions \mathcal{E} in Eq. 5 are given by,

$$\mathcal{E}_{\text{edit}} = \frac{1}{\alpha + \frac{1}{2}\beta(1 + \cos(f_i(\mathbf{F}^{\text{gen}}, \mathbf{m}^{\text{gen}}), \text{gc}(f_i(\mathbf{F}^{\text{gud}}, \mathbf{m}^{\text{gud}}))))}, f_i \in \{f_{\text{local}}, f_{\text{global}}\}, \quad (12)$$

$$\mathcal{E}_{\text{content}} = \frac{1}{\alpha + \frac{1}{2}\beta(1 + \cos(f_{\text{local}}(\mathbf{F}^{\text{gen}}, \mathbf{m}^{\text{share}}), \text{gc}(f_{\text{local}}(\mathbf{F}^{\text{gud}}, \mathbf{m}^{\text{share}}))))}, \quad (13)$$

where \mathbf{F} denotes the features and the masked features are $f_{\text{local}} = \mathbf{F}_t[\mathbf{m}]$ and $f_{\text{global}} = (\sum \mathbf{F}_t[\mathbf{m}]) / \sum \mathbf{m}$. The mask for the edited region, \mathbf{m}_{edit} is aligned with the mask in the generated and reference images, which are denoted as \mathbf{m}^{gen} and \mathbf{m}^{gud} , respectively. $\mathbf{m}^{\text{share}}$ denotes the shared region between the source and reference, e.g., background. $\text{gc}(\cdot)$ is the gradient clipping operation [59]. The energy function $\mathcal{E}_{\text{edit}}$ gets larger when the cosine similarity between the masked features of the generated and reference gets larger.

F Design Choices

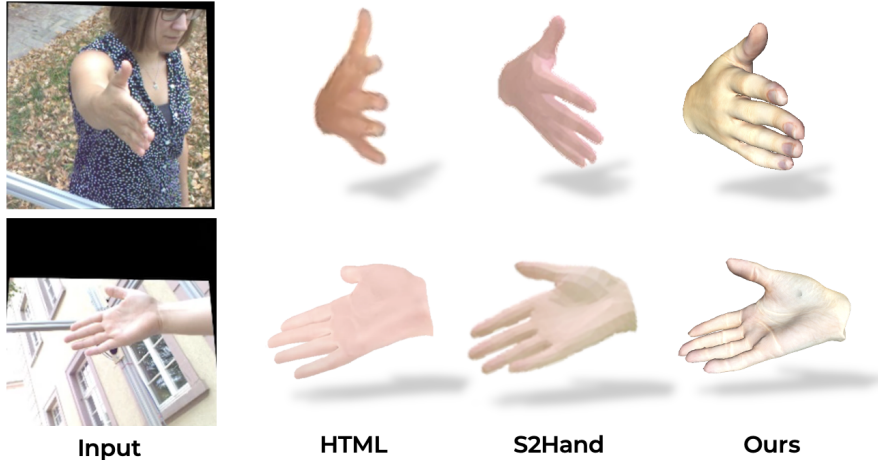


Figure 17: Comparisons of the single image hand textured reconstruction results. The superior quality of ours, which follows [41] and [102], motivated us to use it, other than the alternatives, i.e., HTML [69] and S²Hand [15].

Our method performs "putting objects in people's hands" with a single image input only. This simple input allows us to work with one of the most widely accessible input – image. However, this brings an unique challenge of turning a single image into a high quality 3D representation. There have been a few previous works which tried *single image to textured 3D hand*. HTML [69] introduced this task many year ago. S²Hand [15] improved the training of such 3D hands with self-supervised learning. After that, NIMBLE [41] was introduced, which considered biometric bones and muscles and greatly increased the resolution of the hand mesh. Then, some works [102] tried to build a textured hand

model using the NIMBLE. We found our high demand for a quality 3D avatar for hands to be a compelling motivation of applying the [102] to our hand reconstruction pipeline. The comparison is depicted in Fig. 17

G Implementation Details

We use 0.1 for the scaling range k . We initialize the transformation of the object by overlapping the centers of the hand and object at the center and scaling the object by the predicted shape code. We used the pre-trained HAT [14] to perform Super Resolution on FreiHAND into 896×896 . For the 2D keypoints in 5, we depend on the Mediapipe [49]. We used Stable Diffusion 1.5 [71] as the backbone of the DiffEditor [60]. We empirically selected $\eta_1 = 0.4$ and $\eta_2 = 0.2$. When making the \mathbf{h}_c , we threshold the distance between hand and object by 1cm. We used [102], which is based on the biometric hand parameterized model [41], for acquiring the hand 3D model from a single image. The reason for the design choice of this hand 3D model is described in Sec. F.

H Computational Resources

The Object Selection Network was trained for 12 hours on two RTX 3090 gpus. The inference of our model consists of the object selection time, the Objaverse fetching time, the optimization time, and the final editing time. Apart from the editing, it took us, in average, 56s for an input on one RTX 3090 gpu. The time can vary depending on the Internet speed, and we tested our model with a network of around 865 Mbps. The overall inference time comparisons are listed in Tab. 4. Although our method adds extra time for object selection and 3D grasping, the large improvement upon other methods on the results could justify the cost.

I Limitations

Limitations The performance of our method depends on the effectiveness of the off-the-shelf single image textured reconstruction model and the 2D keypoint estimation model. Moreover, our current method does not support open-vocabulary object categories, nor infinite number of objects. We believe that although the use of large-scale 3D models provided us with objects with high details, the growing community of shape generation and texture synthesis methods would be able to substitute such large, but predefined 3D database in our future works. Plus, incorporating human affordance prior into our test-time optimization will be beneficial, given the rising popularity of large pretrained models that may better understand human behaviors.